# UNIVERSITY OF AMSTERDAM

## The Evolution of Relativistic Binary Progenitor Systems

Francischelli, G.J.; Wijers, R.A.M.J.; Brown, G.E.

# THE EVOLUTION OF RELATIVISTIC BINARY PROGENITOR SYSTEMS

G. J. FRANCISCHELLI, R. A. M. J. WIJERS, AND G. E. BROWN
Department of Physics and Astronomy, State University of New York, Stony Brook, NY 11794; francis@mail.astro.sunysb.edu,
rwijers@sbast3.ess.sunysb.edu, popenoe@nuclear.physics.sunysb.edu

## ABSTRACT

Relativistic binary pulsars, such as B1534+12 and B1913+16, are characterized by having close orbits with a binary separation of $\sim 3\ R_\odot$. The progenitor of such a system is a neutron star, helium star binary. The helium star, with a strong stellar wind, is able to spin up its compact companion via accretion. The neutron star's magnetic field is then lowered to observed values of about $\sim 10^{10}$ G. Since the pulsar lifetime is inversely proportional to its magnetic field, the possibility of observing such a system is thus enhanced by this type of evolution. We will show that a nascent (Crab-like) pulsar in such a system can, through accretion-braking torques (i.e., the "propeller effect") and wind-induced spin-up rates, reach periods that are close to observed values. Such processes occur within the relatively short helium star lifetimes. Additionally, we find that the final outcome of such evolutionary scenarios depends strongly on initial parameters, particularly the initial binary separation and helium star mass. Indeed, the majority of such systems end up in the pulsar "graveyard," and only a small fraction are strongly recycled. This fact might help to reconcile theoretically expected birth rates with limited observations of relativistic binary pulsars.

*Subject headings:* binaries: close — pulsars: general — stars: neutron

## 1. INTRODUCTION

Two of the five known high-mass binary pulsar systems (HMBPs)—PSR B1913+16 (Hulse & Taylor 1975) and PSR B1534+12 (Wolszczan 1990)—have short orbital periods ($\sim 10$ hr). Such systems, on their eventual mergers, are considered to be important sources of gravitational wave radiation, which may be measured by the next generation of ground-based detectors. As a result, it becomes desirable to understand the evolutionary processes that lead to their formation. Note that we do not consider PSR B2127+11C (Prince et al. 1991), which resides in the globular cluster M15; globular cluster sources may have completely different evolution mechanisms that are dominated by dynamical interactions.

The link between relativistic binaries and their original O/B main-sequence progenitor systems are believed to be wide high-mass X-ray binaries (or Be/HMXBs). The standard evolutionary scenario following the X-ray phase (Bhattacharya & van den Heuvel 1991; van den Heuvel & van Paradijs 1993) predicts that the neutron star enters the hydrogen envelope of its giant companion. Common envelope (CE) evolution ensues as the compact object spirals in, creating dynamical friction and ultimately expelling the envelope. The orbit is then tightened, leaving a helium star, neutron star binary. However, Chevalier (1993) showed that a neutron star in CE evolution would likely form a black hole. Brown (1995) confirmed this scenario, showing that hypercritical accretion forces $\geq 1\ M_\odot$ onto the neutron star, sufficient to form a black hole.

Brown's alternate scenario for the formation of relativistic binaries involves, instead, a double helium star binary (Brown 1995; Wettig & Brown 1996). If the progenitor O/B supergiants are initially very close in mass (within 4%), the two stars will burn helium at the same time. Thus, it is possible for the neutron star to avoid moving through the envelope of the secondary. Although CE evolution takes place, it does so with two helium stars. Furthermore, a natural explanation is given as to why the pulsar, which gains mass by accretion, is the heavier star in the binary. Such a result is supported by observations. Notice that either scenario leads to a neutron star, helium star binary as an intermediate stage. Thus, the evolutionary scenario discussed here is generally applicable.

It should be emphasized that we lack a complete understanding of the evolutionary history of neutron stars, even with regard to their measured/inferred properties such as spin period and magnetic field. In this paper, we use only simple physical arguments and empirical models to explain such phenomena. Our description of the response of the neutron star spin to torques and mass flows is fairly detailed and probably not far from correct. The magnetic field evolution, however, is very poorly understood, and in this first study we only use one very simple heuristic description of this process. Therefore, many aspects of the evolutionary scenario presented here are preliminary in nature, and on further refinements in the theory, our model should be adjusted. However, we feel that the simplified model used here already yields useful insights.

We take the Crab pulsar (PSR 0531−21) as the standard prototype for young neutron stars. Thus, we model the pulsar born into the binary as having a strong magnetic field, $(3–10) \times 10^{12}$ G, and a short spin period, 30–50 ms. However, it should be noted that this long-accepted paradigm for young neutron stars is currently being challenged. Kaspi (2000) points out that alternate pulsar models are being developed in response to direct observations of supernova remnants (SNRs). Indeed, most SNRs differ from the Crab Nebula in that they lack both visible pulsars and a central plerion. Additionally, there is mounting evidence for magnetars in the study of anomalous X-ray pulsars and soft gamma repeaters. On the other hand, if our model of accretion-driven magnetic field decay (see § 2.5) is correct, there is insufficient time for a magnetar field ($B_i \gtrsim 10^{14}$ G) to decay to the observed HMBP range for our scenario.

Thus, binary magnetars are not considered here as possible progenitors to recycled HMBPs.

We will show that small orbital separations (1–3 $R_\odot$) and strong helium star winds ensure heavy accretion onto the neutron star, causing its magnetic field to decrease by 2 orders of magnitude and spinning it up further. Competing with wind-fed accretion is the so-called propeller effect. This mechanism exerts a spin-down torque on rapidly rotating neutron stars as material is prevented from accreting (Pringle & Rees 1972; Illarionov & Sunyaev 1975; Fabian 1975). We shall see that such a scenario is, indeed, consistent with observations of relativistic binaries such as PSR 1913+16. Note that diminished magnetic field strengths lengthen the observable lifetime of a pulsar ($t_{obs} \propto 1/B$). Thus, an "observability premium" is given to recycled pulsars.

In § 2, we discuss our model of the evolution of a helium star and neutron star in a close binary. Particularly, we examine how the spin period and magnetic field of the neutron star as well as the orbital separation of the system change with time. Since many parameters are involved, an analytic solution is not readily available. Instead, in § 3, we discuss results of a computer code that was set up to analyze the model. Additionally, since initial conditions are not well understood, we also discuss the effect of the variation of parameters on possible outcomes. It is determined that the final outcome of the binary evolution strongly depends on such parameters (particularly initial orbital separation and helium star mass), and furthermore, the number of systems that would lead to an observable, recycled pulsar is limited.

## 2. DESCRIPTION OF THE MODEL

It has been shown (Langer 1989; Woosley, Langer, & Weaver 1993) that when a helium star loses matter from an enhanced stellar wind, the mass-loss rate is dependent on its total mass. We consider, as a first approximation, the expression given by Woosley et al. (1993), i.e., $\dot{M}_{He} = -5 \times 10^{-8}\ M_\odot\ yr^{-1}\ (M_{He}/M_\odot)^{2.6}$.

However, it has recently been argued (Ergma & van den Heuvel 1998; Brown et al. 2001) that this rate is too high by a factor of 2–3. Initially, Ergma & van den Heuvel (1998) found that helium star mass-loss rates must be lowered, at least for the case of progenitors to black hole binaries such as Cygnus X-1. Since stellar black holes in close binaries must necessarily evolve from Wolf-Rayet stars (their hydrogen-rich envelopes easily being stripped away), the presence of strong helium stellar winds implies a progenitor main-sequence mass exceeding 40 $M_\odot$ for the case of Cygnus X-1, but applying the wind-loss rates of Woosley et al. (1993) yields a remnant with mass less than 4.25 $M_\odot$, contradicting observations. Thus, they conclude that real wind losses must be lowered by at least a factor of 2. Brown et al. (2001) independently argue in favor of reduced mass-loss rates. Their conclusion is supported by polarization measurements of Thomson scattering in helium stars as well as the observed scaling of mass-loss rates with orbital period changes (St.-Louis et al. 1993; Moffat & Robert 1994). Using polarization measurements of V444 Cygni ($M_{He} = 9.3\ M_\odot$), St.-Louis et al. (1993) found $\dot{M}_{He} = 0.75 \times 10^{-5}\ M_\odot\ yr^{-1}$. (Note that they use a slightly different value for the terminal wind velocity; see eq. [5].) Extrapolating this rate to all helium star masses and assuming the same scaling as in Woosley et al., we therefore find

$$\dot{M}_{He} = (-2.5 \times 10^{-8}\ M_\odot\ yr^{-1})\left(\frac{M_{He}}{M_\odot}\right)^{2.6}. \quad (1)$$

The helium star nuclear burning lifetime is also dependent on its total mass. In an approximation to evolutionary calculations made by Paczyński (1971) and Habets (1986), Pols et al. (1991) estimate a functional form for helium star lifetimes as

$$T_{He} = \begin{cases} (1.148 \times 10^7\ yr)\left(\dfrac{M}{M_\odot}\right)^{-1.6}, & 1.6 < M/M_\odot < 4.8\ , \\ (2.37 \times 10^6\ yr)\left(\dfrac{M}{M_\odot}\right)^{-0.6}, & M/M_\odot > 4.8\ . \end{cases}$$
$$(2)$$

Habets (1986) has shown that helium stars with $M \leq 2.2$ $M_\odot$ become white dwarfs and, thus, are not considered here. Also note that since we assume the progenitor to our model to be a double helium star binary, we only use half of the total helium star lifetime, given by equation (2), in our calculations. In § 3.2, we discuss the strengths and weaknesses of this approximation.

We then look to the question of how much of the ejected helium star matter is actually accreted onto its compact companion ($M_x$). The captured mass fraction $f_c$ is defined as the fraction of mass captured by the neutron star's gravitational field and is given by $f_c = -\dot{M}_{cap}/\dot{M}_{He}$, where $\dot{M}_{cap}$ is the mass capture rate. Note that since $\dot{M}_{He}$ is negative, $f_c$ is always greater than or equal to zero. Similarly, the accreted mass fraction $f_a$ is given by the fraction of mass captured that is actually accreted onto the surface of the compact star. Here $f_a = \dot{M}_x/\dot{M}_{cap}$. Since matter cannot be accreted faster than the Eddington limit, we define $f_a = 1$ if $\dot{M}_{cap} < \dot{M}_{Edd}$ but $f_a = \dot{M}_{Edd}/\dot{M}_{cap}$ for super-Eddington transfers. In sum, we see

$$\dot{M}_e = -f_c\ f_a\ \dot{M}_{He}\ . \quad (3)$$

Additionally, one may define the parameter $\alpha$ as the total fraction of matter that is lost from the system. In that case, $\alpha = 1 - f_c\ f_a$.

Assuming a standard Keplerian orbit with binary separation $a$, the neutron star moves relative to the helium star with a circular orbital velocity

$$v_x = \left[\frac{G(M_{He} + M_x)}{a}\right]^{1/2}, \quad (4)$$

The helium star wind velocity at the position of the neutron star can be estimated to be (see, e.g., Castor 1970)

$$v_w = v_\infty\left(1 - \frac{R_{He}}{a}\right). \quad (5)$$

In an approximation to numerical work done by Habets (1986) and Paczyński (1971), we estimate that the helium star radius is given by $R_{He}/R_\odot = 0.22(M_{He}/M_\odot)^{0.6}$ and $v_\infty \approx 2000$ km s$^{-1}$. Generally, the helium stellar wind will move out radially, orthogonal to $v_x$, so that the pulsar experiences the wind moving at a relative velocity of $v_r = (v_w^2 + v_x^2)^{1/2}$.

The value for the He star radius given in equation (5) needs to be adjusted when taking into account later stages

of evolution. At the onset of core carbon ignition, a helium star may expand to a red giant (Habets 1986; Woosley et al. 1993). This is especially true for low-mass stars ($M_{He} < 3$ $M_\odot$), for which expansion can lead to $R_{He} > 200$ $R_\odot$ (Habets 1986). Even for intermediate mass stars (i.e., $3 \lesssim M_{He}/M_\odot \lesssim 4.5$), some post–main-sequence expansion can occur, and it is necessary to extrapolate red giant radii from Habets (1986) and incorporate them into our model.

Adopting the standard accretion mechanism (Bondi 1952), we assume incoming matter gets captured near the so-called accretion radius $R_g$. This is defined as the point at which the wind velocity (relative to the neutron star) is equal to the escape velocity of infalling matter. Thus,

$$R_g = \frac{2GM_x}{v_r^2} . \tag{6}$$

It should be noted that Bondi (1952) defines the accretion radius as $R_g = 2GM_x/(v_r^2 + c_s^2)$, where $c_s$ represents the speed of sound in the plasma. However, in massive stars $v_w \gg c_s$, so equation (6) is a valid approximation.

Finally, we can use geometry to estimate the captured mass fraction $f_c$. We determine it to be the fraction of a sphere of radius $a$ that occupies the area enclosed by the accretion radius of the neutron star, i.e., $f_c = \pi R_g^2/4\pi a^2$. With equation (6), this becomes

$$f_c = \frac{G^2 M_x^2}{a^2(v_x^2 + v_w^2)^2} . \tag{7}$$

## 2.1. Orbital Evolution

In order to determine how the orbital separation changes with time, one needs to model how angular momentum is transferred in the binary. Neglecting spin angular momentum and assuming circular Keplerian orbits, one finds $J_{orb} = \mu a^2 \omega$, where $\omega = [G(M_x + M_{He})/a^3]^{1/2}$ and $\mu$ is the reduced mass. Recalling that $\dot{M}_x = (\alpha - 1)\dot{M}_{He}$ and differentiating, one can easily show

$$\frac{\dot{a}}{a} = \frac{2\dot{J}_{orb}}{J_{orb}} - \frac{2\dot{M}_{He}}{M_{He}} \left[ 1 + (\alpha - 1)\frac{M_{He}}{M_x} - \frac{\alpha}{2}\left(\frac{M_{He}}{M_x + M_{He}}\right) \right].$$
$$\tag{8}$$

Since matter is being lost from the system, it is clear that total angular momentum will not be conserved. It is then necessary to make some assumptions about how angular momentum is transferred from one star to another. Reasonably, one could expect that the actual mass being passed from the helium star to the neutron star (i.e., $f_c dM_{He}$) is transferred conservatively. We then assume that the fraction $(1 - f_c)dM_{He}$ will leave the system with the specific angular momentum of the helium star $\hat{j}_{He}$. Thus, $dJ_i = (1 - f_c) dM_{He}\hat{j}_{He} = (1 - f_c)dM_{He}(M_x/M_{tot})^2 a^2 \omega$. Similarly, we expect that $f_c(1 - f_a)dM_{He}$ leaves the system with the specific angular momentum of the neutron star $dJ_f = f_c(1 - f_a)dM_{He}(M_{He}/M_{tot})^2 a^2 \omega$. Together, these assumptions yield a differential equation for the orbital angular momentum of the system $\dot{J}_{orb} = \dot{J}_i + \dot{J}_f$,

$$\frac{\dot{J}_{orb}}{J_{orb}} = \frac{\dot{M}_{He}}{M_x + M_{He}} \left[ (1 - f_c)\frac{M_x}{M_{He}} + f_c(1 - f_a)\frac{M_{He}}{M_x} \right]. \tag{9}$$

Defining the mass ratio $q \equiv M_x/M_{He}$ and combining

equations (8) and (9), we find

$$\frac{\dot{a}}{a} = \frac{\dot{q}[q - f_c(2 - 2q^2 + f_a q)]}{(q + f_c f_a)q(1 + q)} . \tag{10}$$

## 2.2. Emitter Phase

Initially, the newborn pulsar is characterized by a rapid spin ($P = 30$–$50$ ms) and a strong dipole magnetic field [$B_s \sim (3$–$5) \times 10^{12}$ G]. Its large dipole radiation pressure might then be sufficient to keep the wind plasma from being accreted onto the neutron star. In this phase the compact star will behave like an isolated radio pulsar, spinning down with time as rotational kinetic energy is converted to dipole radiation energy. Such systems have been extensively studied (Gunn & Ostriker 1969; Goldreich & Julian 1969), and we model dipole radiation pressure for a neutron star of radius $R_x$ and spin period $\Omega$ as

$$P_{rad}(r) = \frac{L}{4\pi r^2 c} = \frac{B^2 R_x^6 \Omega^4}{24\pi r^2 c^4} . \tag{11}$$

The *stopping radius* $R_s$ is defined as the point at which dipole radiation pressure is sufficient to balance wind pressure from the helium star (Urpin, Geppert, & Konenkov 1998). If the stopping radius is greater than the accretion radius, then the neutron star will behave like an isolated emitter, spinning down via the Gunn-Ostriker mechanism. However, if $R_g > R_s$, then it is possible for the pulsar to accrete. We estimate wind pressure to be given by $P_w \sim \rho_w v_w^2$, where $\rho_w$, the plasma density, is approximately given by $\rho_w \approx |\dot{M}_{He}|/4\pi a^2 v_w$. Finally, setting $P_w = P_{rad}(R_s)$, we get an expression for the stopping radius

$$R_s = \sqrt{\frac{B^2 R_x^6 a^2 \Omega^4}{6c^4 |\dot{M}_{He}| v_w}} . \tag{12}$$

Note that since no accretion may take place at this point ($f_c = f_a = 0$), the pulsar magnetic field will remain constant (see eq. [18]). The spin period $P = 2\pi/\Omega$ will increase according to the standard relation (Gunn & Ostriker 1969)

$$P\dot{P} = \left(\frac{16\pi^2 R_x^6}{3Ic^3}\right)B^2 . \tag{13}$$

Here $I = k^2 MR^2$ represents the moment of inertia of the neutron star with $k^2 \sim 0.4$ (Lattimer & Prakash 2001).

## 2.3. The Propeller Phase

According to equation (12), the stopping radius is proportional to the inverse square of the period. Thus, over a relatively short amount of time, the pulsar will spin down sufficiently such that accreting matter may interact with the magnetosphere of the neutron star. Recall that this occurs at the point at which the stopping radius falls inside the accretion radius.

We assume, for simplicity, that the magnetospheric boundary of the neutron star is defined where the ram pressure of infalling matter is balanced by the neutron star's magnetic dipole pressure (Lamb, Pethick, & Pines 1973). Assuming spherical inflow (but see Ghosh & Lamb 1979a, 1979b), the magnetospheric radius is thus

$$R_m = \left(\frac{B^4 R_x^{12}}{8GM_x \dot{M}_{cap}^2}\right)^{1/7} . \tag{14}$$

Once matter couples to the neutron star's magnetic field, the interaction's effect on the overall spin evolution depends on the balance between centrifugal and gravitational accelerations. If the pulsar rotation is initially too fast, the neutron star will eject infalling plasma, propelling it away tangentially while simultaneously losing angular momentum in the process. This "propeller" effect (Pringle & Rees 1972; Illarionov & Sunyaev 1975) can be parameterized by a *fastness parameter* $\omega_s \equiv \Omega/\Omega_K(R_m)$, where $\Omega_K(R_m) = (GM_x/R_m^3)^{1/2}$ is the Keplerian angular velocity at the magnetospheric boundary. Clearly, for a fastness parameter greater than unity, the propeller mechanism is initiated. An alternate, yet equivalent, parameterization of the propeller effect can be defined by introducing the *corotation radius* $R_c$, which is defined such that $\Omega \equiv \Omega_K(R_c)$. For $r > R_c = (GM_x/\Omega^2)^{1/3}$, corotating matter is accelerated outward by centrifugal forces, but for $r < R_c$, corotating matter can accrete. Since matter is forced to corotate when it couples to the pulsar magnetosphere ($r = R_m$), the propeller effect occurs for all $R_m > R_c$. The resulting angular momentum loss (and associated increase in spin period) can be represented by a propeller torque, $N_{prop}^J = I\dot{\Omega} = -\dot{M}_{cap} R_m v_{esc}(R_m) = -\dot{M}_{cap}(2GM_x R_m)^{1/2}$. Consequently, the spin rate decreases according to the relation

$$\frac{\dot{P}}{P^2} = \frac{\dot{M}_{cap}}{2\pi I}\sqrt{2GM_x R_m} \ . \quad (15)$$

It is instructive to note that it is also possible to use energy methods to determine the propeller torque. Over time, rotational kinetic energy of the neutron star will be transmitted through shocks to the wind plasma falling near the magnetospheric boundary (Fabian 1975). Consequently, this gas will heat up and be dispersed when it attains escape velocity $[V \sim V_{esc} = (2GM_x/R_m)^{1/2}]$. Thus, we find $\dot{E} = I\Omega\dot{\Omega} = -\frac{1}{2}\dot{M}_{cap} V_{esc}^2 = -GM_x \dot{M}_{cap}/R_m$. Hence, $N_{prop}^E = I\dot{\Omega} = -GM_x \dot{M}_{cap}/R_m \Omega = -[GM_x \dot{M}_{cap}/R_m \Omega_k(R_m)]\omega_s^{-1}$.

On examination of the two possible propeller torques, we see

$$N_{prop}^E = -\frac{\dot{M}_{cap}}{\omega_s}\sqrt{GM_x R_m} = \frac{N_{prop}^J}{\sqrt{2}\omega_s} \ . \quad (16)$$

Thus, for extremely fast rotators, it is much more difficult for an energy propeller to change the spin period of the neutron star significantly. The physical reason for this is that in the energy propeller, the matter only just gets enough energy to escape, whereas in the angular momentum propeller at high fastness, it receives much more energy before leaving. The reality of the magnetospheric interaction is a very complex magnetohydrodynamic problem, so it is hard to say which mechanism is inherently more accurate. Therefore, we use both the energy and angular momentum propellers and compare results.

## 2.4. *Accretion*

For a fastness parameter less than unity, corotating matter is able to accrete to the surface of the neutron star. At this point, since the helium star wind carries angular momentum, we expect the pulsar spin period to decrease over time. Thus, the pulsar is said to be *recycled*.

It is not initially clear whether spherical or disk accretion will dominate over the course of the helium star burning time. Shapiro & Teukolsky (1983) argue that if the intrinsic angular momentum per unit mass of accreted gas $\hat{j}_{acc}$

exceeds the specific angular momentum of an element in a circular Keplerian orbit near the magnetospheric radius $\hat{j}_K(R_m) = (GM_x R_m)^{1/2}$, then disk accretion will dominate. Otherwise, we may treat the mass transfer as being (nearly) spherical. Thus, the necessary prerequisite for a disk to form is $\hat{j}_{acc} \geq \hat{j}_K$, where it may be shown (Shapiro & Teukolsky 1983) that $\hat{j}_{acc} = (1/2a)v_x R_g$ and $v_x$ and $R_g$ are given by equations (4) and (6), respectively.

For spherical accretion ($\hat{j}_{acc} < \hat{j}_K$), the spin-up torque is simply given by $N_{acc} \equiv \dot{J}_{acc} = \dot{M}_x\hat{j}_{acc}$. However, when modeling disk accretion, it then becomes desirable to include the effects of magnetic torques within the disk on the overall spin rate (viscous torques may be ignored here). This complex problem was first discussed by Ghosh & Lamb (1979a, 1979b), who found that for slow rotators ($\omega_s \ll 1$), magnetic coupling may enhance spin-up torques by as much as 40%. For $\omega_s \lesssim 1$, the opposite is true, and magnetic effects might actually *oppose* the spin-up. Following Ghosh & Lamb, we define, for disk accretion, $N_{acc} = n(\omega_s)\dot{M}_x\hat{j}(R_m)$, where the dimensionless coefficient, valid for $0 \leq \omega_s \leq 0.9$, is given by

$$n(\omega_s) \approx \frac{1.39\{1 - \omega_s[4.03(1-\omega_s)^{0.173} - 0.878]\}}{(1-\omega_s)} \ . \quad (17)$$

## 2.5. *Magnetic Field Decay*

Next, we discuss the evolution of the neutron star's magnetic field. Recent observations and analyses seem to strongly indicate that mass accretion in binary systems is directly correlated with magnetic field decay in neutron stars (but see Wijers 1997). Although there exist many possible accounts of physical mechanisms that would explain this phenomenon (Konar & Bhattacharya 1997), here we rely on the empirical model of Shibazaki et al. (1989) and leave a more detailed analysis of accretion-driven magnetic field decay for later work.

For typical initial values of dipole magnetic field strengths, i.e., $B_{12} \sim 1$–10, it was determined that one can make the following empirical approximation to magnetic field evolution (Shibazaki et al. 1989):

$$B(t) = \frac{B_0}{1 + (\Delta M_x/M_s)} \ . \quad (18)$$

Here $M_s \sim 12.5 \times 10^{-6} \ M_\odot$ is a typical scaling parameter. This parameter has been set to qualitatively agree with the inferred dipole magnetic fields of low-mass X-ray binaries (LMXBs). Over their lifetimes, LMXBs can accrete up to $\sim 0.1 \ M_\odot$ and have typical magnetic fields on the order of $5 \times 10^8$ G. Assuming an initial field strength of $B_0 \sim 5 \times 10^{12}$ G, we see that equation (18) roughly gives the desired result.

## 2.6. *Valving and Equilibrium*

As we have shown, the line of demarcation between spin-up (propeller effect) and spin-down (accretion) phases of evolution is parameterized by the fastness parameter $\omega_s$. For a very fast rotator, $\omega_s \gg 1$ and the spin period increases with time as the magnetic field remains constant. However, as the neutron star spins down, the corotation radius $R_c \propto P^{2/3}$ will increase. Since the propeller phase continues, the corotation radius will continue to increase until it is finally

greater than the magnetospheric radius, given by equation (14). At this point, the neutron star will allow corotating matter to fall to its surface, and the accretion phase begins.

However, once accreting, the magnetic field begins to decay. From equations (14) and (18), we see that $R_m$ is, roughly, a monotonically decreasing function of time and that as accretion continues, the magnetospheric radius diminishes, possibly allowing the propeller phase to resume.

In sum, we expect a kind of oscillation or "valving" to occur between accretion and propeller phases of the neutron star's evolution, until equilibrium is restored. For spherical mass transfer at equilibrium, the corotation radius should coincide with the magnetospheric boundary. In this case, one can estimate the equilibrium spin period of the neutron star:

$$P_{eq} = (17.3 \text{ ms})\left(\frac{\dot{M}_x}{\dot{M}_{Edd}}\right)^{3/7} B_{10}^{6/7} R_6^{18/7} \left(\frac{M_x}{M_\odot}\right)^{-5/7} . \quad (19)$$

So, for a canonical neutron star accreting spherically at the Eddington limit, $P_{eq} = (13.6 \text{ ms})B_{10}^{6/7}$. Since the magnetic field is brought down with each cycle of accretion, $P_{eq}$ is brought down as well.

The equilibrium point for disk accretion is generally more complicated. On examination of the Ghosh & Lamb function (eq. [17]), we find that $n(\omega_s)$ is undefined for $\omega_s = 1$. In this case, we define the critical ratio $\omega_c \equiv 0.5050$. Since $n(\omega_c) \sim -1$ and for all $\omega_s \geq \omega_c$ magnetic torques are sufficient to force the neutron star to spin down, we *define* $\omega_s = \omega_c$ as the turnover from a propeller to an accretor; i.e., we define all $n(\omega_s \geq \omega_c) = -1$.

## 3. RESULTS OF THE NUMERICAL CALCULATIONS

As discussed in § 1 and expanded on in the previous section, there are several parameters that need to be accounted for in order to evolve the binary system with time. We are thus led to several coupled differential equations for which there is no analytic solution. Instead, we now discuss the results of a computer code set up to analyze the model.

At each time step within the total helium burning time (eq. [2]), the stopping radius, accretion radius, magnetospheric radius, and fastness parameter were calculated in order to determine the predominant phase of the evolution (i.e., emitter, propeller, or accretor). The differential equations of § 2 were then solved numerically using a simple Euler scheme, and the calculated parameters were appropriately updated. In fact, because many transitions between evolutionary stages are discontinuous, higher order integration schemes will fail.

Initial conditions such as stellar masses, neutron star spin period, magnetic field strength, and orbital separation for relativistic binary progenitors are largely unknown, so the simulation was run for a wide range of values. Specifically, the initial helium star mass was varied in the range 2.2 $M_\odot \leq M_{He} \leq 15\ M_\odot$. Helium stars with masses below the lower limit tend to evolve into white dwarfs (Habets 1986), whereas stars with masses far above 15 $M_\odot$ will more likely dissociate the binary on supernova and are rare in any case. Neither possibility would lead to relativistic binary systems. It has been shown (Brown et al. 2001) that because of their strong stellar wind, naked helium stars in this mass range generally end their lives as neutron stars and not as black holes. Similarly, since we are interested in the progenitors of

close binaries, the initial orbital separation was chosen to have the (somewhat arbitrary) maximum value of 10 $R_\odot$.

The criterion determining the minimum orbital separation was defined such that the helium star stays within its Roche lobe, i.e., $R_{He} < R_L$. If a helium star were allowed to expand beyond its Roche lobe, unstable mass transfer would commence. Such a scenario would generally not lead to the formation of an HMBP and is thus excluded. Eggleton (1983) has shown that for a mass ratio $q$ (eq. [10]), the Roche-lobe radius of a star is given by

$$\frac{R_L}{a} = \frac{0.49}{0.6 + q^{2/3} \ln(1 + q^{-1/3})} \equiv f(q) . \quad (20)$$

From equation (20), we see that $a_{min} = R_{He}/f(q)$ and is, therefore, a function of helium star mass. On the helium main sequence, $R_{He}/R_\odot = 0.22(M_{He}/M_\odot)^{0.6}$, but (§ 2) low-mass stars may further expand to a red giant after the core helium burning phase (Habets 1986; Woosley et al. 1993). Thus, it is likely that low-mass helium stars ($M_{He}$) in close binaries will undergo unstable mass transfer after the main-sequence phase of its evolution, possibly leading to an additional spiral-in.

We used the Crab pulsar (PSR 0531−21) as a prototype nascent neutron star (see § 1 and Kaspi 2000 for some possible exceptions to this assumption). Canonical values were given for neutron star masses, radii, and moments of inertia (1.4 $M_\odot$, $10^6$ cm, and $\sim 10^{45}$ g cm$^2$, respectively). Initial spin periods ranged from 30 to 50 ms, and initial dipole field strengths varied in the range (1–10) × $10^{12}$ G. We note that varying the initial magnetic field to the so-called magnetar range does not allow sufficient time for the observed recycling seen in HMBPs using our present magnetic decay model. Thus, magnetars are not considered here. Additionally, since $P_i$ is generally unknown, one might assume that a much larger range of initial spin periods should be used. In fact, such variations have little effect on the outcome of calculated final spin periods and magnetic field strengths. For example, allowing $P_i = 500$ ms yields essentially the same results as the $P_i = 50$ ms case for all initial helium star masses and orbital separations. Actually, the propeller effect is slightly weaker for long initial periods than for short periods but only for the case of minimal recycling. In the strong recycling case (i.e., those neutron stars that are seen as HMBPs), there is essentially no dependence on initial spin period. Thus, our restriction to Crab-like pulsars seems valid.

### 3.1. Some Characteristic Case Studies

Here we first examine four possible cases of evolutionary scenarios in order to illustrate some basic trends of our model. Then, in § 3.2 we discuss a more systematic variation of parameters and their effect on the measured properties of the pulsar. Several plots of the time evolution of spin period and magnetic field under various conditions follow, and certain general trends are evident. A sharp rise in spin period with time (with no corresponding change in magnetic field) indicates that the primary factor dominating the evolution is the propeller effect. However, when the spin period lengthens to some critical value, the propeller mechanism gives way to accretion. At this point, the period and magnetic field strength both decrease with time.

For sufficiently large initial binary separations and/or low helium star masses, accretion may not occur at all

during the total helium burning time. In such a case, the dipole field of the neutron star remains constant, and its overall spin period actually *increases* with time because of the propeller effect and electromagnetic spin-down. Many times, this spin-down is sufficiently large to put the neutron star in the pulsar graveyard.

Figure 1 examines the time evolution of the pulsar spin period and magnetic field for both the energy and angular momentum propellers (see § 2.3) under typical conditions. Initial parameters are given by $M_{\mathrm{He},i} = 4.0\ M_\odot$, $B_i = 5.0 \times 10^{12}$ G, $P_i = 50.0$ ms, and $a_i = 1.50\ R_\odot$. The total helium burning time is calculated, using equation (2), to be $6.246 \times 10^5$ yr. Clearly, the final results and overall evolution are sensitively dependent on the type of propeller mechanism used. For the case of the angular momentum propeller, the neutron star quickly enters the accretion phase at $t = 2.42 \times 10^4$ yr. Consequently, it ends up with a short final period (99.74 ms) and low magnetic field strength ($4.169 \times 10^{10}$ G). Thus, the given initial conditions, coupled with the *J*-propeller mechanism, are sufficient to recycle the pulsar. Things are quite different for the energy propeller, however. From Figure 1, we see that the neutron star never accretes at all and that the magnetic field remains constant throughout the evolution. Weak torquing inhibits the rapid spin-down seen for the *J*-propeller. Instead, the period remains roughly constant with $P_f = 121.1$ ms. Additionally, we see that although the angular momentum propeller reaches a period close to the equilibrium period (eq. [19]) early in its evolution ($\sim 4 \times 10^5$ yr), the *E*-propeller never does. For both cases, the helium star loses $0.4848\ M_\odot$ by a steady wind, and as anticipated, most of this mass is lost. The neutron star accretes $1.494 \times 10^{-3}\ M_\odot$ for the *J*-propeller, while mass transfer is completely noncon-

servative for the *E*-propeller. Note that for this low-mass helium star, mass capture is always sub-Eddington and $f_a = 1$ for all time. We have only considered the main-sequence evolution of the helium star here and note (see discussion below eq. [20]) that on core carbon ignition, another spiral-in may occur. Thus, it is unclear at this point whether or not such a scenario will lead to an HMBP or, possibly, a black hole binary (Fryer & Kalogera 1997). Finally, we see that the type of propeller mechanism has little effect on the widening of the orbit ($a_f = 1.644$ and 1.645 $R_\odot$, respectively).

Figure 2 illustrates the case in which a low-mass helium star (3 $M_\odot$) is in a relatively wide orbit ($a_i = 8\ R_\odot$). The initial properties of the neutron star are otherwise identical to the previous case. Here we see that accretion does not set in until $t \sim 5.7 \times 10^5$ yr for the angular momentum propeller, while the energy propeller again does not accrete at all over the total evolution time of $9.897 \times 10^5$ yr. For the first phase of the evolution, the weak wind of the helium star is insufficient to push past the stopping radius of the neutron star. The pulsar acts like an emitter, spinning down electromagnetically. Then at $t \sim 4.9 \times 10^4$ yr, the concavity of the curve in the $P$ versus $t$ diagram changes. At this point, the neutron star has spun down sufficiently for the helium star wind to begin to interact with its magnetosphere. However, the pulsar is still a fast rotator, and the propeller phase commences.

The type of propeller mechanism determines the next stage of the binary's evolution. For the case of the angular momentum propeller, the neutron star rapidly spins down to a maximum pulse period greater than 43 s. At $t = 5.65 \times 10^5$ yr, accretion finally begins, but equilibrium is never achieved. Only $9.880 \times 10^{-6}\ M_\odot$ is actually
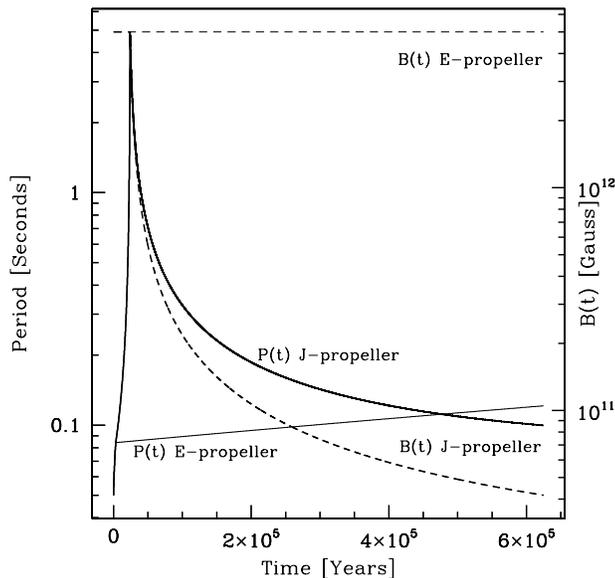


FIG. 1.—Time evolution of the pulsar spin period (*solid lines*) and magnetic field (*dashed lines*) over the main-sequence lifetime of the companion He star for both the angular momentum and energy propellers. For both cases, $B_i = 5 \times 10^{12}$ G, $P_i = 50$ ms, and $a_i = 1.50\ R_\odot$. The initial helium star mass is $4.0\ M_\odot$. For the *J*-propeller, we see evidence of recycling with $P_f = 99.74$ ms and $B_f = 4.169 \times 10^{10}$ G. The neutron star accretes $1.494 \times 10^{-3}\ M_\odot$ over an evolution time of $6.246 \times 10^5$ yr. For the *E*-propeller, weak torquing inhibits a rapid spin-down, and consequently, there is no accretion. The final spin period is 121.1 ms, while the magnetic field does not change.
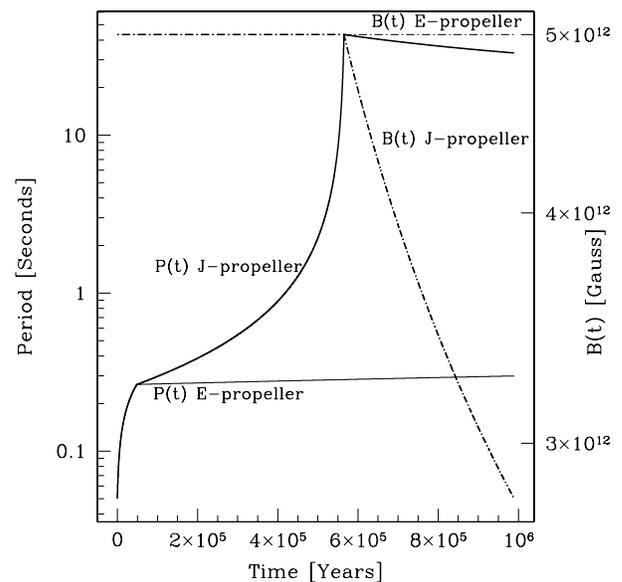
FIG. 2.—Main-sequence evolution for the case of a low-mass helium star (3 $M_\odot$) in a wide orbit ($a_i = 8\ R_\odot$). Other initial conditions are the same as in Fig. 1. For the *J*-propeller, the pulsar will end up in the graveyard with a final spin period of 33.1 s. Only $9.88 \times 10^{-6}\ M_\odot$ is accreted onto the surface of the neutron star ($\Delta M_{\mathrm{He}} = -0.3636\ M_\odot$), and there is little field decay ($B_f = 2.798 \times 10^{12}$ G). For the *E*-propeller, once again, there is no accretion as evidenced by the constant magnetic field. Here the final spin period is 298.9 ms, and the neutron star is observable as a radio pulsar. For both scenarios, the total evolution time is $9.897 \times 10^5$ yr, and the orbit widens until $a_f = 8.720\ R_\odot$.

accreted to the surface ($\Delta M_{\mathrm{He}} = -0.3636 \ M_{\odot}$), and the final spin period and magnetic field strength of the neutron star are 33.14 s and $2.798 \times 10^{12}$ G, respectively. Clearly the pulsar has entered the graveyard, and this system would not be observed as a relativistic binary. Once again, for the energy propeller, weak torquing prevents significant changes in the spin period, and although the neutron star never accretes at all (magnetic field remains unchanged), the final spin period is 298.9 ms. As a result, the neutron star can be observed as a radio pulsar (yet it is clearly not recycled). For both scenarios, the final orbital separation is 8.720 $R_{\odot}$. In either case, the helium star will undergo significant expansion during the red giant phase of its evolution leading to unstable mass transfer.

Finally, we examine the case in which a massive helium star lies in a close orbit with a neutron star. In this case we expect there to be heavy accretion and recycling. In particular, consider a 12 $M_{\odot}$ helium star in orbit with a canonical neutron star ($P_i = 50$ ms, $B_i = 5 \times 10^{12}$ G) with an initial binary separation of 3.0 $R_{\odot}$. Figure 3 illustrates the resulting evolution of spin and magnetic fields for the angular momentum propeller. We see that there is, indeed, heavy accretion, and after a sharp propeller cycle, equilibrium is achieved at $P_f = 60.41$ ms. Additionally, the neutron star accretes $2.086 \times 10^{-3} \ M_{\odot}$, which is sufficient to bring the field down to $2.993 \times 10^{10}$ G in a time of $2.668 \times 10^5$ yr. The final orbital separation is 3.833 $R_{\odot}$. Little to no expansion is expected here at the onset of carbon ignition. Mass transfer is spherical throughout the evolution. The minimum period of 59.35 ms occurs near $t \sim 2.1 \times 10^5$ yr, where steady accretion gives way to valving. At this point, the period slowly increases and closely tracks the (time-dependent) equilibrium period. The energy propeller again prohibits accretion onto the neutron
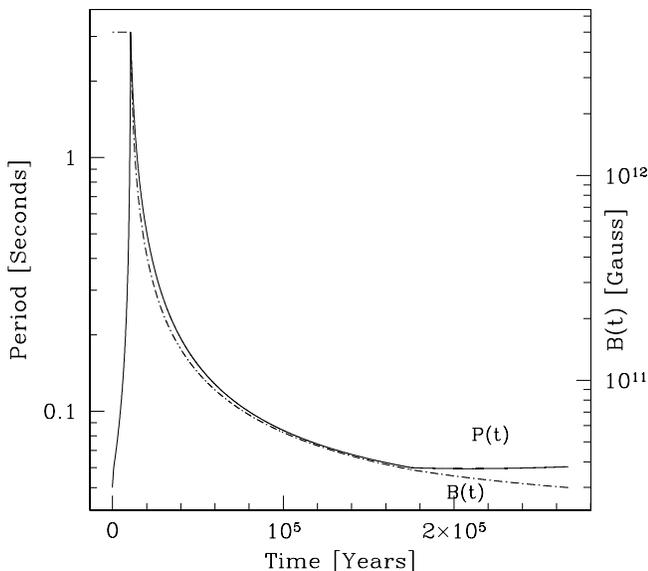
star. Through electromagnetic spin-down and propeller torque, the pulsar gradually increases its spin to a final period of 83.71 ms. All of the helium star wind matter (2.944 $M_{\odot}$) is lost, while the magnetic field remains constant.

For sufficiently heavy accretion, it is possible that slight changes in initial orbital separation may result in significant differences in the neutron star's spin period evolution. Consider the case of a 10 $M_{\odot}$ helium star in orbit about a neutron star with initial magnetic field $7.5 \times 10^{12}$ G and initial spin period 35 ms. Assume an angular momentum propeller effect only. Figure 4 shows the resulting time evolution for $a_i = 1.95$ and 2.05 $R_{\odot}$. We find that the binary in the closer initial orbit actually has a *longer* final spin period. Such a result seems counterintuitive and needs to be examined more closely.

When $a_i = 2.05 \ R_{\odot}$, accretion is spherical throughout the mass transfer phase, lasting from $t = 6.1 \times 10^3$ yr until the time of the helium star's supernova at $t = 2.98 \times 10^5$ yr. The final, equilibrium spin period is 48.4 ms. However, for the case when $a_i = 1.95 \ R_{\odot}$, accretion changes from disk-type to spherical. The short, initial, electromagnetic spin-down phase is nearly identical for both cases, as is the initial propeller phase. Then, at $t \sim 5.6 \times 10^3$ yr, spherical accretion begins. This continues uninterrupted until $t \sim 4.2 \times 10^4$ yr. At this point, a second, smaller, propeller phase begins and continues until $t = 4.25 \times 10^4$ yr. Valving and disk accretion set in at this time, allowing the spin period to gradually decrease with time. Finally, at $t = 2.46 \times 10^5$ yr, $\hat{j}_{\mathrm{acc}}$ falls below $\hat{j}_{\mathrm{K}}$, and spherical accretion commences again. This results in a much faster drop in spin period with time. The neutron star spherically accretes until the helium star supernova and the final spin period for this case is 55.0 ms.
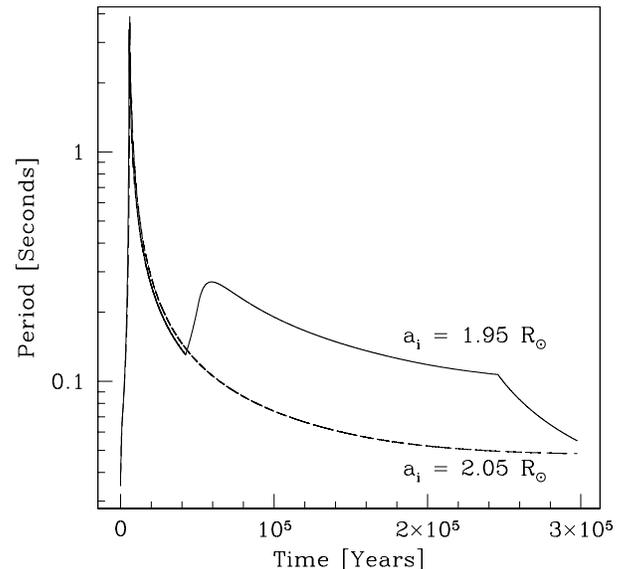
FIG. 3.—Spin and magnetic field evolution for the case $a_i = 3 \ R_{\odot}$ and $M_{\mathrm{He}, \, i} = 12 \ M_{\odot}$ (angular momentum propeller only). All other initial conditions are the same as in previous cases. There is heavy accretion, and after a sharp propeller cycle, the neutron star spins up to an equilibrium period of 60.41 ms. The field strength is, subsequently, lowered to a final value of $2.993 \times 10^{10}$ G in a time of $2.668 \times 10^5$ yr. The final orbital separation is 3.833 $R_{\odot}$. For the $E$-propeller (not shown), there is no recycling and $P_f = 83.71$ ms.

FIG. 4.—Here we see the time evolution of the spin period for a canonical neutron star ($P_i = 35$ ms and $B_i = 7.5 \times 10^{12}$ G) in a close orbit with a 10 $M_{\odot}$ helium star ($J$-propeller). For $a_i = 2.05 \ R_{\odot}$, there is continuous spherical accretion from $t = 6.1 \times 10^3$ until $t_f = 2.98 \times 10^5$ yr. The final equilibrium spin period is 48.4 ms. However, by slightly changing the initial conditions, such that $a_i = 1.95 \ R_{\odot}$, the time evolution becomes quite different. Here spherical accretion dominates from $5.6 \times 10^3$ until $4.2 \times 10^4$ yr. This leads to a second (smaller) propeller phase and a cycle of disk accretion. Finally, at $t = 2.46 \times 10^5$ yr, accretion again becomes spherical and $P_f = 55$ ms.

### 3.2. Observed Parameter Dependence on Orbital Separation and Helium Star Mass

Next we examine the results of a contour plot that parameterizes the final spin period and magnetic field as functions of initial orbital separation and helium star mass. Standard initial values were again chosen for the neutron star with $M_{x, i} = 1.4 \, M_\odot$, $B_i = 5 \times 10^{12}$ G, and $P_i = 50$ ms (see § 3). As discussed in § 3, the initial helium star mass range is $2.2 \, M_\odot \leq M_{He, i} \leq 15 \, M_\odot$, whereas the initial orbital separation varied in the range $a_{min} \leq a_i \leq 10 \, R_\odot$. Here $a_{min}$ is defined to be $R_{He}/f(q)$ (eq. [20]). For low-mass stars, $R_{He}$(red giant) $\gg R_{He}$(main sequence), leading to a nearly vertical cutoff below $M_{He} \lesssim 4.5 \, M_\odot$. The output of the contour plots representing the angular momentum propeller and energy propeller appear in Figures 5 and 6, respectively.

From the slope of the contours in Figure 5a, it is clear that for close orbits, the final spin period most strongly depends on the initial orbital separation and less on the helium star mass. However, for wider (initial) orbits, both parameters are important for the final outcome.

If neutron stars act as angular momentum propellers, then for any orbit with initial separation greater than $\sim 6$ $R_\odot$, the pulsar will not only be unrecycled but it will sit in the graveyard as well. Therefore, there is a strong constraint placed on progenitors of relativistic binary pulsars such as $1913+16$.

Recall that observable pulsar lifetimes are proportional to $1/B$. Thus, one expects an "observability premium" for low-field, fast rotators; i.e., because of longer lifetimes outside the graveyard, one should expect to observe a higher proportion of such systems. Indeed, this is true of the two relativistic binaries (three including $2127+11$C). It seems that, on examination of Figure 5a, in order to bring the field below $5 \times 10^{10}$ G ($0.01 B_i$), the initial binary separation must be a *maximum* of $\sim 4 \, R_\odot$. Additionally, if one wishes to observe a system with spin periods on the order of 50 ms, even closer orbits are necessary, with $a_0 \sim 2$–$3 \, R_\odot$, and this is only true for the most massive of helium stars, i.e., those with $M_{He, i} > 8 \, M_\odot$. Thus, for angular momentum–type propellers, we conclude that only a minute portion of the overall parameter space represented in Figure 5 will produce relativistic binary pulsars such as PSRs $1913+16$ and $1534+12$.

The parameter space of final outcomes is much more highly constrained for the energy propeller (Figs. 6a and 6b) than for the angular momentum propeller. It seems, from examining the spin period contour plot in Figure 6a, that it is extremely difficult (if not impossible) for a neutron star to spin down into the graveyard by the E-propeller mechanism. Even in the weak wind, wide orbit limit, $P_f$ never rises much higher than $\sim 0.5$ s. At the other extreme, we find that it is also very difficult to force the neutron star to accrete at all for this scenario. Figure 6b shows that mass transfer, parameterized by magnetic field decay, occupies only a tiny portion of $M$-$a$ space. From equation (16), we see that the propeller torque is inversely proportional to the fastness parameter. Thus, unlike the J-propeller, fast rotators are unable to easily change their spin period. Thus, one may conclude that the energy propeller is highly inefficient at recycling pulsars.

This characteristic becomes a significant factor in determining whether an E-propeller will accrete at all or not. As with the J-propeller, slightly changing the initial conditions
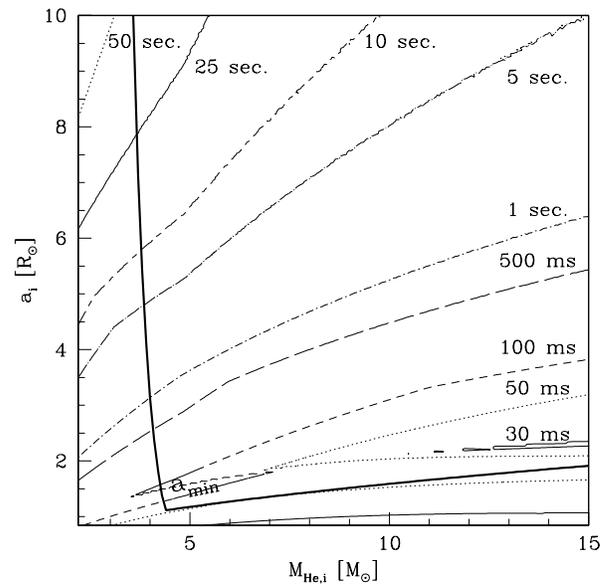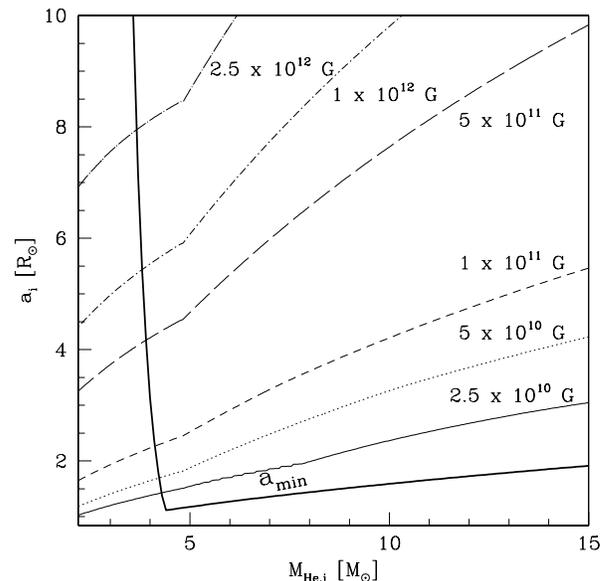


FIG. 5a



FIG. 5b

FIG. 5.—Contour plots of (a) final spin period and (b) final magnetic field strengths as a function of initial separation and helium star mass for the angular momentum propeller effect. Initial values are given using the Crab pulsar (PSR $0531-21$) as a prototype. Therefore, we have set $B_i = 5 \times 10^{12}$ G and $P_i = 50$ ms. Variation of these parameters do not change the final outcome much. The initial helium star mass varied in the range 2.2 $M_\odot \leq M_{He} \leq 15 \, M_\odot$, and the initial orbital separation range was $a_{min} \leq a \leq 10 \, R_\odot$. The $a_{min}$ line is defined by $a_{min} \equiv R_{He}/f(q)$ (see text). The lower right-hand portion of the graph indicates heavy recycling, whereas the upper left-hand contours represent neutron stars that have spun into the graveyard.

(particularly the initial orbital separation) may make a profound difference in the final outcome of the pulsar's evolution (although for different reasons). The result of this condition is the dense band of contours near the $a_{min}$ line in Figure 6a. For a specific example of why this occurs, consider a 6 $M_\odot$ helium star orbiting a neutron star with initial parameters $B_i = 4 \times 10^{12}$ G and $P_i = 70$ ms. Figure 7a shows a plot of final spin period as a function of initial separation in the range $a_{min} = 1.27 \, R_\odot \leq a_i \leq 2.5 \, R_\odot$.
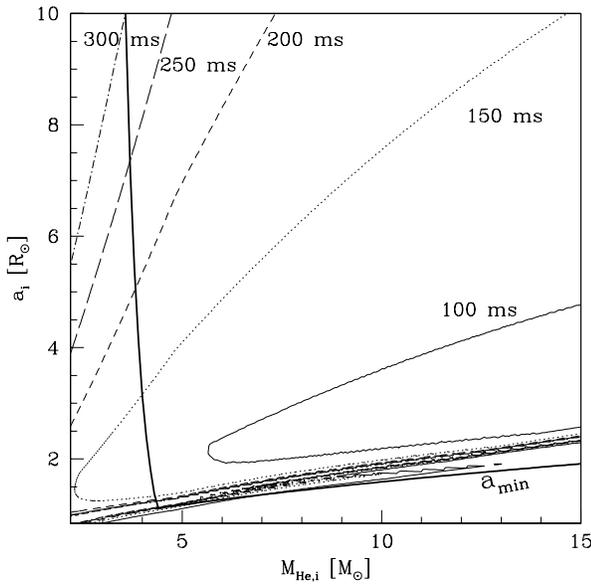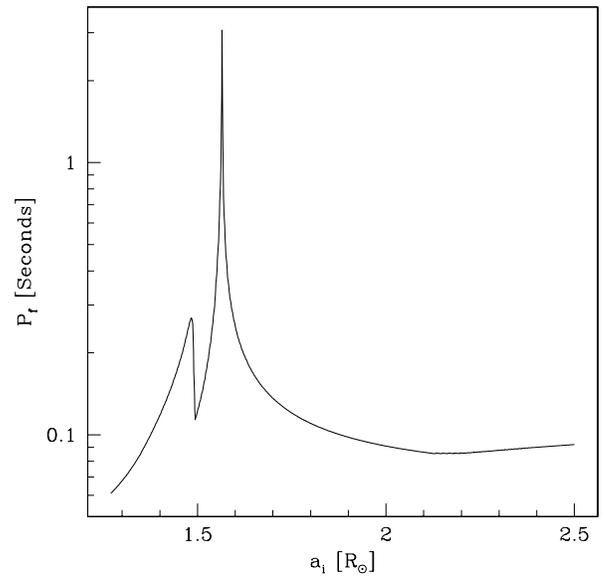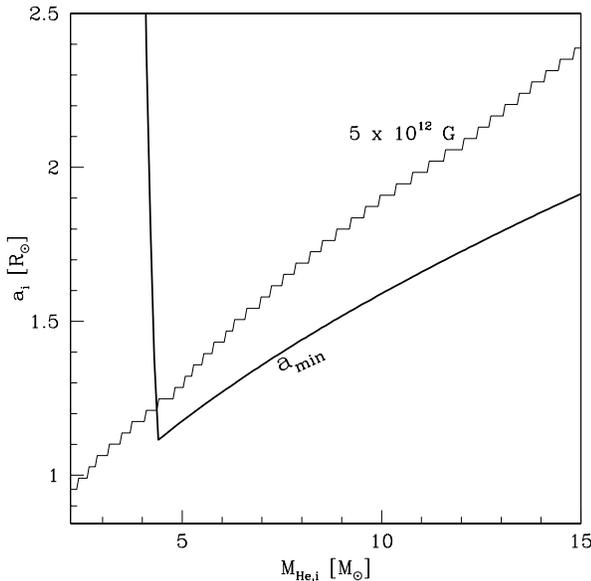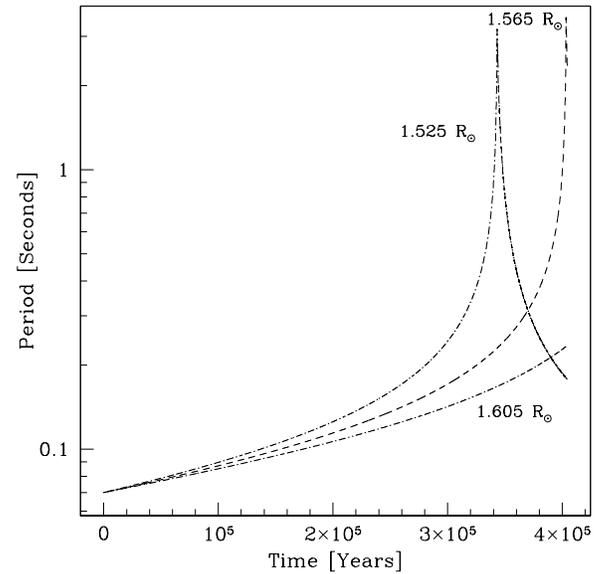
FIG. 6a

FIG. 7a

FIG. 6b

FIG. 7b

FIG. 6.—Contour plots of (a) final spin period and (b) final magnetic field as functions of initial orbital separation and helium star mass for the energy propeller. Initial conditions and parameter space are the same as for the angular momentum propeller. Note that final values are much more strongly constrained, and it seems, it is very difficult for the $E$-propeller mechanism to either spin the neutron star into the graveyard or sufficiently recycle it to form a relativistic binary such as PSR 1913+16. In Fig. 6a we see that final spin periods near the $a_{\min}$ line are sensitively dependent on the initial conditions (see text for an explanation). From Fig. 6b we find that accretion and subsequent magnetic field decay is absent for the vast majority of the parameter space in the case of the $E$-propeller.

FIG. 7.—(a) Plot of final spin period as a function of initial separation in the range $1.27\ R_\odot \le a_i \le 2.5\ R_\odot$ (energy propeller, $B_i = 4 \times 10^{12}$ G, $P_i = 70$ ms, $M_{\mathrm{He},i} = 6\ M_\odot$). A sharp maximum occurs at the point $a_i = 1.567$ $R_\odot$ where $P_{\max} = 3.06$ s. For $a_i > 1.6\ R_\odot$, $P_f$ falls dramatically to about $\sim 85$ ms at $a_i = 2.1\ R_\odot$. At this point, the final period gradually rises again with increasing separation. (b) Plot of the time evolution of the spin period for three different initial orbital separations—1.525, 1.565, and 1.605 $R_\odot$. See text for details.

A sharp peak exists at the point $a_i = 1.567\ R_\odot$. Here $P_f$ reaches a maximum value of 3.063 s. For $a_i > 1.6\ R_\odot$, $P_f$ falls dramatically to a level of about $\sim 85$ ms at $a_i = 2.1\ R_\odot$. At this point there is a much more gradual increase in final spin period with increasing separation. What causes the sudden shift in final spin period? As Figure 7b shows, a slight change in initial orbital separation will have an effect

on the fastness parameter and, thus, the overall evolution of the propeller phase. Here we examine the time evolution of the spin period for the three different initial orbital separations—1.525, 1.565, and 1.605 $R_\odot$. As the initial orbital separation increases, the propeller torque will decrease by a small amount, and as a result, it takes longer for the neutron star to reach its maximum period. For $a_i = 1.525\ R_\odot$, the spin period reaches a maximum of 3.09 s at $t = 3.43 \times 10^5$ yr. Afterward, the accretion phase begins and continues until the end of the helium star lifetime at

$4.044 \times 10^5$ yr, where $P_f = 177.7$ ms. A relatively long accretion phase allows the magnetic field to decay to a final value of $1.358 \times 10^{11}$ G. So, we see a slightly recycled neutron star for the given initial conditions. Changing the initial separation to $1.565\ R_\odot$ increases the fastness parameter and, consequently, decreases the propeller torque. Now the peak does not occur until nearly the end of the evolution ($t = 4.03 \times 10^5$ yr). Since there is little time for the accretion phase, the magnetic field does not change much ($B_f = 2.6 \times 10^{12}$ G), and the final spin period is 2.33 s. Thus, the pulsar winds up in the graveyard and is not observable. Finally, by increasing the initial separation to $1.605\ R_\odot$, we can eliminate the accretion phase altogether. Here the pulsar peak never occurs, and the neutron star cannot be recycled. The magnetic field remains constant throughout the evolution ($P_f = 234.9$ ms).

We note that such variations in final pulsar properties are greatly affected by the total helium burning time. Recall (§ 2) that the total evolution time varies between zero (when the two progenitors have equal mass and, thus, finish burning helium simultaneously) and the maximum given by equation (2). In our model, we approximated the helium burning time to be half that given by equation (2) and note that such an approximation *usually* does not affect the outcome. Typically, recycling occurs early in the total evolution of the binary, especially for the $J$-propeller, and massive helium stars (see, e.g., Fig. 3). Since we expect such a scenario to be favored in the production of relativistic HMBPs such as PSR 1913+16, our approximation seems to hold for such cases. However, on reexamination of Figure 7b, we see that varying the evolution time under certain circumstances can have a profound effect on the outcome. One must keep this in mind when interpreting our results.

Next we consider the nonrelativistic HMBPs such as PSR J1518+4904 (Nice, Sayer, & Taylor 1996) and the newly discovered PSR J1811−1736 (Lyne et al. 2000). Of all five known HMBPs, 1518+4904 is the most recycled ($P = 40.94$ ms, $\log B = 9.1$). However, it resides in a relatively wide binary with an orbital period of 8.634 days ($a \sim 25\ R_\odot$). Similarly, PSR J1811−1736, recently discovered by the Parkes Multibeam Pulsar Survey (Lyne et al. 2000), is another wide HMBP with a very eccentric orbit. With a measured orbital period of 18.8 days, J1811−1736 shows signs of recycling ($P = 104$ ms, $\log B = 10.2$). Unfortunately, our model cannot account for such properties.

From Figure 5a ($J$-propeller), we see that if $a_i > 6\ R_\odot$, the pulsar is destined to end up in the graveyard. Even for the most massive helium star companions, the neutron star will never accrete, and instead, a large propeller torque will sharply increase its spin period. Such a trend diminishes for $a_i \gg 10\ R_\odot$ since, for very wide binaries, $R_g > R_s$ for most (if not all) of the evolution. The helium star wind is too weak to interact with the neutron star's magnetosphere at such separations, and the pulsar spins down electromagnetically. Thus, we would expect that J1518+4904 would not be observable nor would it undergo magnetic field decay.

Although the evolutionary history of PSRs 1518+4904 and 1811−1736 is unknown, it is clear that our model does not account for all possibilities. We therefore must assume that their evolution was different than the other HMBPs. One possible evolutionary scenario that may account for the observed properties of the two wide HMBPs is reverse case C mass transfer (Kippenhahn & Weigert 1967). Since low-mass helium stars tend to have significantly extended envelopes (Habets 1986), even an initially wide binary may undergo sufficient mass transfer to initiate recycling after the helium shell-burning stage. Assuming the neutron star survived the resulting spiral-in phase, it may be possible to end up with a recycled pulsar in a wide binary. Thus, we find that two possible improvements to our current model would be an accurate treatment of case C mass transfer and a more detailed physical model of magnetic field decay.

## 4. CONCLUSION

Relativistic binary pulsars, such as B1534+12 and B1913+16, are characterized by having close orbits ($a \sim 3\ R_\odot$) with recycled pulse periods and magnetic fields ($P \sim 30$–60 ms, $\log B \sim 10$). Two cases of a wide HMBPs (J1518+4904 and J1811−1736) exist.

We assume that wind-fed mass transfer is responsible for recycling the observable neutron star in an HMBP. In lieu of a more detailed physical mechanism, we use the empirical model of Shibazaki et al. (1989) to account for magnetic field decay. Such a model assumes that changes in the pulsar magnetic field are proportional to the amount of mass accreted to its surface. We find that for close initial orbits ($a_i \sim 2$–3 $R_\odot$) and an initial helium star mass in the range $8\ M_\odot \lesssim M_{\mathrm{He},i} \lesssim 15\ M_\odot$, we are able to reproduce the observed spin periods, orbital separations, and magnetic fields for HMBPs 1913+16 and 1534+12. Brown et al. (2001) find that helium stars in this mass range will generally end their lives as neutron stars. Whereas such high-mass He stars are relatively rare, they do not undergo a significant red giant phase after helium shell burning. Finally, we note that with such a high initial helium star mass, a kick velocity on supernova would be required if the system is to remain bound. This is consistent with earlier calculations made by Burrows & Woosley (1986).

Our model was unable to account for the properties of PSRs 1518+4904 and 1811−1736, and we speculate that another mechanism such as reverse case C mass-transfer (not modeled in this paper) is responsible for their properties.

Cycles of accretion coupled with the propeller effect allow the neutron star to come to be recycled in a time consistent with helium star nuclear lifetimes. Of the two possible propeller mechanisms proposed, only the angular momentum propeller is efficient at recycling the HMBP progenitors to observed properties. Since pulsar lifetimes are inversely proportional to their magnetic fields ($t_{\mathrm{obs}} \propto 1/B$), recycling and magnetic field decay lengthen the observable lifetime for a neutron star. Thus, an "observability premium" is introduced for relativistic binary pulsars. Furthermore, we also find that the final outcome of the binary evolution strongly depends on initial conditions (particularly $M_{\mathrm{He},i}$ and $a_i$). In some cases, there is quite a sensitive dependence, especially during the propeller phase. Thus, the number of possible observable systems are constrained to a small region of the overall parameter space of initial conditions.

REFERENCES

Bhattacharya, D., & van den Heuvel, E. P. J. 1991, Phys. Rep., 203, 1
Bondi, H. 1952, MNRAS, 112, 195
Brown, G. 1995, ApJ, 440, 270
Brown, G. E., Heger, A., Langer, N., Lee, C. H., Wellstein, S., & Bethe, H. A. 2001, NewA, 6, 457
Burrows, A., & Woosley, S. E. 1986, ApJ, 308, 680
Castor, J. I. 1970, MNRAS, 149, 111
Chevalier, R. 1993, ApJ, 411, L33
Eggleton, P. P. 1983, ApJ, 268, 368
Ergma, E., & van den Heuvel, E. P. J. 1998, A&A, 331, L29
Fabian, A. C. 1975, MNRAS, 173, 161
Fryer, C., & Kalogera, V. 1997, ApJ, 489, 244
Ghosh, P., & Lamb, F. K. 1979a, ApJ, 232, 259
———. 1979b, ApJ, 234, 296
Goldreich, P., & Julian, W. 1969, ApJ, 157, 869
Gunn, J. E., & Ostriker, J. P. 1969, Nature, 221, 454
Habets, G. M. H. J. 1986, A&A, 167, 61
Hulse, R. A., & Taylor, J. H. 1975, ApJ, 195, L51
Illarionov, A. F., & Sunyaev, R. A. 1975, A&A, 39, 185
Kaspi, V. M. 2000, in IAU Colloq. 177, Pulsar Astronomy: 2000 and Beyond, ed. M. Kramer, N. Wex, & R. Wielebinski (ASP Conf. Ser. 202; San Francisco: ASP), 485
Kippenhahn, R., & Weigert, A. 1966, Z. Astrophys., 65, 251
Konar, S., & Bhattacharya, D. 1997, MNRAS, 284, 311

Lamb, F. K., Pethick, C. J., & Pines, D. 1973, ApJ, 184, 271
Langer, N. 1989, A&A, 220, 135
Lattimer, J. M., & Prakash, M. 2001, ApJ, 550, 426
Lyne, A. G., et al. 2000, MNRAS, 312, 698
Moffat, A. F. J., & Robert, C. 1994, ApJ, 421, 310
Nice, D. J., Sayer, R. W., & Taylor, J. H. 1996, ApJ, 466, L87
Paczyński, B. 1971, Acta Astron., 21, 417
Pols, O. R., Coté, J., Waters, L. B. F. M., & Heise, J. 1991, A&A, 241, 419
Prince, T. A., Anderson, S., B., Kulkarni, S. R., & Wolszczan, A. 1991, ApJ, 374, L41
Pringle, J. E., & Rees, M. J. 1972, A&A, 21, 1
Shapiro, S. L., & Teukolsky, S. A. 1983, Black Holes, White Dwarfs, and Neutron Stars: The Physics of Compact Objects (New York: Wiley)
Shibazaki, N., Murakami, T., Shaham, J., & Nomoto, K. 1989, Nature, 342, 656
St.-Louis, N., Moffat, A. F. J., Lapointe, L., Efimov, Y. S., Shakhovskoy, N. M., Fox, G. K., & Piirola, V. 1993, ApJ, 410, 342
Urpin, V., Geppert, U., & Konenkov, D. 1998, MNRAS, 295, 907
van den Heuvel, E. P. J., & van Paradijs, J. 1993, Sci. Am., 269 (11), 38
Wettig T., & Brown, G. E. 1996, NewA, 1, 17
Wijers, R. A. M. J. 1997, MNRAS, 287, 607
Wolszczan, A. 1990, IAU Circ., 5073, 1
Woosley, S. E., Langer, N., & Weaver, T. A. 1993, ApJ, 411, 823